Agricultural Water Management 121 (2013) 73–80

Contents lists available at SciVerse ScienceDirect

Agricultural Water Management

journal homepage: www.elsevier.com/locate/agwat

Solute transport in a loamy soil under subsurface porous clay pipe irrigation

A.A. Siyal [a,*], M. Th. van Genuchten [b], T.H. Skaggs [c]

[a] Department of Land and Water Management, Sindh Agriculture University Tandojam, Pakistan
[b] Department of Mechanical Engineering, Federal University of Rio de Janeiro, UFRJ, Rio de Janeiro, RJ, 21945-970, Brazil
[c] U.S Salinity Laboratory, USDA-ARS, 450 W. Big Springs Rd., Riverside, CA 92507, USA

ARTICLE INFO

Article history:
Received 28 July 2012
Accepted 10 January 2013

Keywords:
Soil salinization
Subsurface irrigation
Okra
Model prediction
HYDRUS-2D

ABSTRACT

Subsurface porous clay pipe irrigation is widely considered to be a very promising method for small-scale irrigation in arid regions. Unfortunately, salt accumulation at and near the soil surface using this method may affect germination of direct-seeded crops. Predicting salt movement and accumulation with clay pipe irrigation will allow producers to anticipate the need for leaching to control salinity in the soil root zone. The HYDRUS-2D model was used to simulate the accumulation of salt from a subsurface clay pipe irrigation system, installed at 30 cm depth, during the growing season of okra (*Abelmoschus esculentus*) irrigated with water having a salinity of 1.1 dS m^{-1}. The loamy soil profile had an initial salinity of 2.3 dS m^{-1}. Predicted electrical conductivity (EC_e) values at the end of the growing season correlated significantly (R^2 = 0.952) with measured saturated paste EC_e data obtained at the end of the field experiments. Salinity was found to be relatively low around the pipes, but increased with distance away from the pipes. Measured and predicted soil salinity levels were especially higher above the clay pipes. Our results indicate that proper management of salt accumulation is vital for sustainable crop production whenever subsurface irrigation systems are being implemented.

1. Introduction

Chronic water shortages in arid regions of the world are compelling farmers to adopt more efficient irrigation methods for sustainable crop production. While in many developed countries high-tech micro-irrigation methods such as sprinkler and drip irrigation are used increasingly, many farmers in developing countries are reluctant to adopt these methods due to their high initial cost of installation and costly maintenance. Traditional irrigation methods such as subsurface pitcher and porous clay pipe irrigation (Ashrafi et al., 2002; Qiaosheng et al., 2007; Siyal et al., 2009) are often preferred by poor farmers in small scale irrigation projects because of their low cost and high irrigation efficiency. Subsurface clay pipe irrigation may be used to improve irrigation uniformity and water use efficiency in a number of different cropping systems. The method allows one to supply the required amount of water by seepage from below the soil surface to the crop at the right place and the right time. This should reduce water losses by evaporation and deep percolation while increasing crop yield and quality.

In subsurface porous clay pipe irrigation, water and solutes not only spread downward and sideways but also move upward due to capillarity and surface evaporation, thus causing salts to accumulate at or near the soil surface. The accumulated salts may be harmful to crops that are subsequently grown at the site, especially directly seeded crops because of their sensitivity to high levels of salinity during germination and establishment (Hussain et al., 1997; Mer et al., 2000; Roberts et al., 2009). Salt accumulation during subsurface clay pipe irrigation is a particular concern in arid regions where annual potential evapotranspiration (*ET*) is much higher than precipitation. Thus, special management techniques are needed to prevent salt accumulation and the resulting harmful effects on germination or seed emergence (Hanson and Bendixen, 1995; Hanson, 2003).

The design and management of subsurface porous clay pipe irrigation systems requires an understanding of water and solute distribution patterns in the soil around the pipes (Siyal and Skaggs, 2009). Optimal management of salt accumulation during and following porous clay pipe irrigation is especially important for high-value crops that are often salt-sensitive. Understanding patterns of salt accumulation at the end of the growing season enable one to foresee a possible need to leach accumulated salts from the near surface by surface flooding or some other method. This understanding may result from a combination of well-designed field experiments and numerical modeling.

* Corresponding author. Tel.: +92 3353340405; fax: +92 222765300.
E-mail addresses: siyal@yahoo.com (A.A. Siyal), rvangenuchten@hotmail.com (M.Th. van Genuchten), Todd.Skaggs@ars.usda.gov (T.H. Skaggs).

0378-3774/$ – see front matter © 2013 Elsevier B.V. All rights reserved.
http://dx.doi.org/10.1016/j.agwat.2013.01.005

Numerical models are now widely used to simulate the flow of water and the transport of solutes in soils (Šimůnek and Bradford, 2008). The HYDRUS-2D software (Šimůnek et al., 1999; Šimůnek and van Genuchten, 2008) is a numerical model capable of simulating many vadose zone flow and transport processes subject to a wide range of boundary conditions and irrigation regimes. In the present study, the ability of HYDRUS-2D to predict the salt distribution after a full cropping season was determined using correlations between model-predicted and field-measured values of the electrical conductivity of the soil saturation extract (EC_e). The data pertain to a subsurface clay pipe field experiment carried out in South-East Pakistan on a medium-textured soil cropped with okra. In a previous study, Siyal and Skaggs (2009) showed that HYDRUS-2D provided excellent predictions of observed wetting patterns in the same soil after 5 days of irrigation using the same porous clay pipe irrigation system. The specific objectives of this study were to predict EC_e values at the end of the okra cropping season, and to correlate the model-predicted EC_e values with the actual EC_e values in order to determine the accuracy of HYDRUS-2D model predictions.

2. Methods and materials

A subsurface irrigation system with baked porous clay pipes was installed in an area of 500 m^2 (20 m × 25 m) at the experimental field of the Faculty of Agricultural Engineering, Sindh Agriculture University Tandojam, Pakistan (Fig. 1). The site is located at 25°25′28” N, 68°32′25” E, about 26 m above mean sea level. The clay pipe irrigation system was very similar to the system previously described in detail by Siyal and Skaggs (2009). Pipes 20 m long were buried at a depth of 30 cm, with a spacing of 1 m. The pipes were formed by cementing together segments having a length of 40 cm and an outside diameter of 13.1 ± 0.2 cm (Fig. 1). More details are given by Siyal and Skaggs (2009).

One of the installed irrigation pipes was chosen at random for field characterization measurements (the eighth out of 25 installed pipes). At three random locations along the selected pipeline, soil samples were taken on both sides of the pipe, at lateral distances of 20 and 40 cm from the centre of the pipeline, at depths of 0–20, 20–40, 40–60, 60–80 and 80–100 cm. In total, 60 samples were taken (3 locations × 4 distances × 5 depths). These samples showed that the mean initial soil profile EC_e down to a depth of 100 cm was 2.3 ± 0.08 dS m^{-1}. The hydrometer method was used to determine the soil particle size distribution (Craze et al., 2003). The texture of the soil according to the USDA system was found to be mostly loam, with the sand fraction ranging from 38 to 56%, the silt fraction from 27 to 39%, and the clay fraction from 15 to 26% (Table 1). The soil bulk density was determined at several locations down to 100 cm depth using a core sampler with a diameter of 1.5 cm. The bulk density measurements ranged from 1.31 to 1.37 g cm^{-3}. No obvious trend in the bulk density versus depth or across the field was observed; hence we used the average value of 1.34 g cm^{-3} to convert gravimetric water content data into volumetric water contents. The soil was different from that used in the previous study (Siyal and Skaggs, 2009). The van Genuchten-Mualem (VGM) soil hydraulic parameters were estimated from soil textural data and the bulk density using the Rosetta pedotransfer functions (Schaap et al., 2001) as implemented in HYDRUS-2D. Soil texture and related hydraulic properties are given in Table 1.

Laboratory-measured saturated hydraulic conductivities (Abu-Zreig and Atoum, 2004) of the walls of four randomly selected pipes were found to be 0.051, 0.046, 0.055, and 0.048 cm d^{-1}. The average saturated hydraulic conductivity (K_s) value of 0.05 cm d^{-1} was used in the simulations. Other hydraulic parameters of the clay pipe were taken to be: $\theta_s = 0.35$, $\theta_r = 0.042$, $\alpha = 0.000001$ cm^{-1} and $n = 1.3$ (where θ_s and θ_r are the saturated and residual water contents, respectively, and α and n are van Genuchten–Mualem shape parameters). The small value of α ensured that the pipe walls remained saturated during the calculations. We refer to Siyal and Skaggs (2009) for more details about the hydraulic conductivity measurements of the clay pipes.

Tube-well water having an EC_w of 1.1 dS m^{-1} was supplied continuously to the clay pipe laterals throughout the okra growing season at a constant positive pressure head of 100 cm. Okra seeds were drilled in rows separately at a depth 2 cm above the clay pipe laterals using a hand drill on 11 February 2009. At the end of the growing season (12 April 2009), soil samples were taken again from the same locations and depths. Hence, in total 60 soil samples were taken again, which were assumed to represent the entire experimental area. Once brought into the laboratory, the samples were air dried and ground to pass through a 2 mm sieve before preparing saturation pastes and determining EC_e values. Due to the presumed lateral symmetry of the wetted zone, the two salt concentrations for the same depths and distances on both sides of the pipe were averaged for subsequent data analysis. No significant rainfall occurred during the entire growing period to contribute either to irrigation or to leaching of salts from the root zone. The total water applied to okra was 10 cm compared to 50 cm usually required for okra with conventional surface irrigation methods, thus demonstrating the potential saving in water provided by clay pipe subsurface irrigation.

2.1. Numerical simulations

Simulations of water flow and solute transport using HYDRUS-2D were based on the Richards equation for water flow and the equilibrium advection-dispersion equation for solute transport in a two-dimensional variably-saturated medium. The general Richards equation is given by:

$$\frac{\partial\theta}{\partial t} = \nabla\cdot(\mathbf{K}\cdot\nabla h + \mathbf{K}) \tag{1a}$$

which for a two-dimensional isotropic medium such as in our study reduces to

$$\frac{\partial\theta}{\partial t} = \frac{\partial}{\partial x}\left[K(h)\frac{\partial h}{\partial x}\right] + \frac{\partial}{\partial z}\left[K(h)\frac{\partial h}{\partial z}\right] + \frac{\partial K(h)}{\partial z} \tag{1b}$$

where x is the horizontal coordinate (L), z is the vertical coordinate (L), t is time (T), θ is the volumetric water content ($L^3\ L^{-3}$), h is the pressure head (L), and $K(h)$ is the unsaturated hydraulic conductivity function (LT^{-1}). The soil water retention, $\theta(h)$, and hydraulic conductivity, $K(h)$, functions needed in Eq. (1b) were described using the functions of van Genuchten (1980):

$$\theta(h) = \theta_r + \frac{\theta_s - \theta_r}{[1 + |\alpha h|^n]^m} \tag{2}$$

$$K(h) = K_s S_e^{0.5}\left[1 - (1 - S_e^{1/m})^m\right]^2 \tag{3}$$

where θ_r, θ_s, K_s, α and n are soil hydraulic parameters as defined previously, $m = 1–1/n$, and S_e is effective saturation given by

$$S_e = \frac{\theta(h) - \theta_r}{\theta_s - \theta_r} \tag{4}$$

Solute transport was described using the general advection–dispersion equation given by:

$$\frac{\partial\theta c}{\partial t} = \nabla\cdot(\theta\mathbf{D}\cdot\nabla c - \mathbf{q}c) \tag{5}$$

where c is the solution concentration (ML^{-3}), $\mathbf{q}$ is the Darcy–Buckingham water flux vector (LT^{-1}), and $\mathbf{D}$ is the dispersion tensor ($L^2\ T^{-1}$), which was described using standard expressions (e.g., Bear, 1972) in terms of the longitudinal (ε_L) and transverse

Fig. 1. Baked clay pipes and their installation at the experimental field.

Table 1
Soil texture and related hydraulic properties.

Soil depth (cm)	Percentage of soil separates			Soil texture	Dry bulk density (g/cm^3)	Soil hydraulic properties				
	Sand	Silt	Clay			θ_r (cm^3 cm^{-3})	θ_s (cm^3 cm^{-3})	K_s (cm d^{-1})	α (cm^{-1})	n
0–20	38.2	41.6	20.2	Loam	1.31	0.065	0.422	20.80	0.008	1.56
20–40	40.8	40.5	18.7	Loam	1.34	0.061	0.411	19.27	0.008	1.55
40–60	39.5	43.2	17.3	Loam	1.33	0.058	0.407	22.05	0.007	1.57
60–80	45.6	36.3	18.1	Loam	1.34	0.059	0.413	22.77	0.010	1.51
80–100	55.0	26.8	18.2	Sandy loam	1.37	0.058	0.419	31.22	0.016	1.45

(ε_T) dispersivities (L). Eq. (5) holds for non-reactive transport, and hence ignores any sorption or precipitation/dissolution of salts in the profile.

Eqs. (1) and (5) were used to simulate water and salt movement in a vertical cross-section containing a functioning clay pipe. Because of symmetry, only the right side of the vertical cross section was simulated. Hence the computational domain was rectangular except for a section on the left side where the clay pipe was represented on the domain boundary by a half-circle (Figs. 2 and 3). The flow domain and computational grid were the same as those used previously by Siyal and Skaggs (2009).

2.2. Initial and boundary conditions

The initial pressure head distribution in the soil profile was determined from the measured water contents of soil samples taken when the irrigation pipes were installed. These water content measurements were converted to pressure heads using the soil water retention characteristic given by Eq. (2) using the loam soil parameter values listed in Table 1. Consistent with these observed values, the initial pressure head was assumed to increase linearly with depth in the profile, from −1000 cm at the soil surface ($z = 0$) to −600 cm at the bottom ($z = 100$ cm) as shown in Fig. 2. The clay pipe internal boundary nodes were assigned a constant pressure head of 100 cm, being equal to the pressure head imposed during

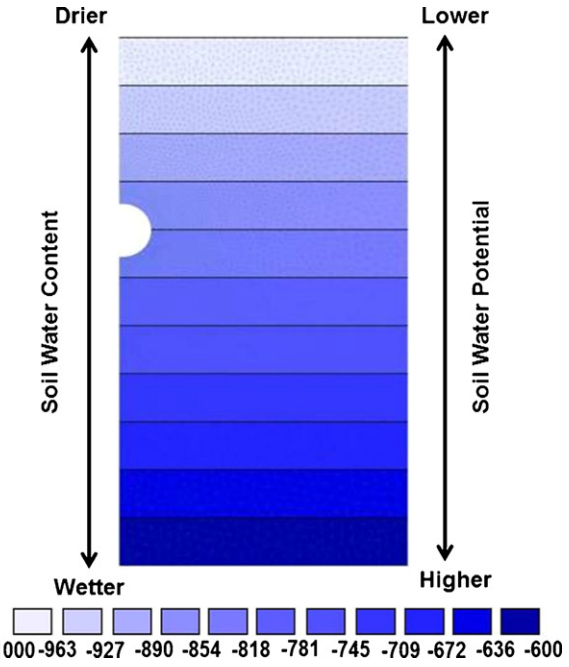

Fig. 2. Linear distribution of initial soil water pressure head (cm) in the soil profile.

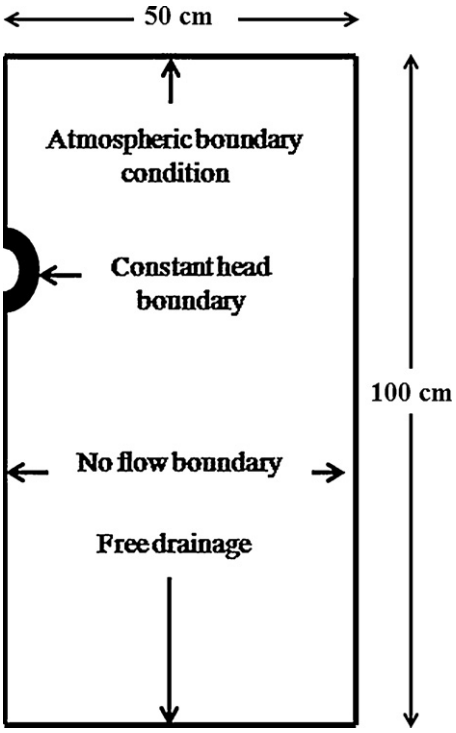

Fig. 3. HYDRUS-2D model domain and boundary conditions.

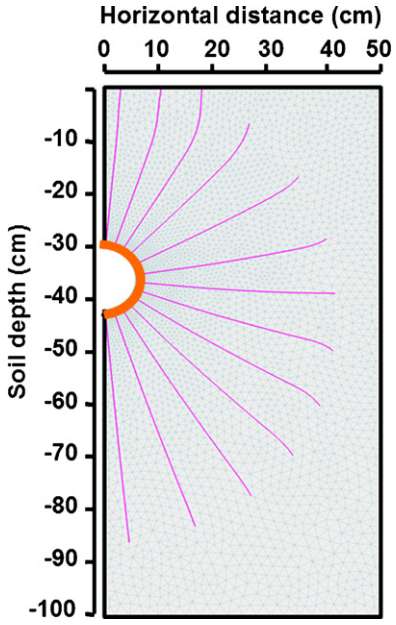

Fig. 4. Trajectories of the water particles originating from clay pipe.

the study. The remaining portion of the left boundary was set as a zero flux condition (due to symmetry in the simulated profile). The surface boundary condition was specified as an "atmospheric boundary condition" (Šimůnek et al., 1999). The potential evaporation and transpiration rates needed for the boundary condition were determined by first calculating a reference evapotranspiration $ET_0(t)$ using the Penman–Monteith method. The potential crop evapotranspiration $ET_p(t)$ was then computed by multiplying the reference evapotranspiration with a crop coefficient (K_c):

$$ET_p(t) = K_c(t) \cdot ET_0(t) \quad (6)$$

$ET_0(t)$ was discretized in daily time steps whereas $K_c(t)$ varied with annual crop growth stage (initial, crop development, mid-season, and late season stages) as described by Allen et al. (1998). Data from Allen et al. (1998) for beans (which are similar to okra) were used to specify the value of K_c during each growth stage. The potential evaporation rate $E_p(t)$ may be estimated from $ET_p(t)$ using an equation of the form:

$$E_p(t) = ET_p(t) \cdot f(t) \quad (7)$$

where $f(t)$ is typically formulated based on Beer's law and the time-variation of the canopy cover (e.g. Pachepsky et al., 2004). Because we did not have data for the time-variation of the canopy cover, we followed (Jiménez-Martinez et al., 2009) and specified $f(t)$ as being a function that decreased sinusoidally from a value of 1 at time $t = 0$ d (planting) to a value of 0 at time $t = 30$ d (full canopy cover). The reasoning for this choice is that initially after planting transpiration would be about zero and thus E_p would be equal to ET_p ($f = 1$), whereas with full canopy (achieved around $t = 30$ d in our case) evaporation would be close to zero ($f = 0$). With ET_p and E_p given by Eqs. (6) and (7), respectively, the potential transpiration $T_p(t)$ was specified by:

$$T_p(t) = ET_p(t) - E_p(t) \quad (8)$$

The bottom boundary was specified as a free drainage (unit gradient) condition while the right boundary was a zero flux condition (Fig. 3).

Soil salinity is typically quantified in terms of the electrical conductivity of the soil water or a soil water extract. Assuming that the soil solution electrical conductivity is simply proportional to the solution salt concentration, transport simulations can be performed in terms of electrical conductivities rather than concentrations Eq. (5). The initial salt concentration of the soil saturation extract was 1440 mg/L, which was converted to electrical conductivity (dS m^{-1}) by dividing by a factor of 640 (U.S. Salinity Laboratory Staff, 1954). This EC_e value (2.3 dS m^{-1}) was then converted to the electrical conductivity that would exist in the soil water (EC_{sw}) at time $t = 0$ (soil sampling time) using the relationship:

$$EC_{sw} = \frac{S_p \rho_b}{100\ \theta \rho_w} EC_e \quad (9)$$

where S_p is soil saturation percentage, ρ_b is soil dry bulk density (g cm^{-3}), ρ_w is density of water (g cm^{-3}), and θ is volumetric soil water content (cm^3 cm^{-3}).

The initial salt concentration of soil in the flow domain was thus set equal to 9.97 dS m^{-1} at the top and 9.26 dS m^{-1} at the bottom during simulations. The conductivity of the irrigation water (EC_{iw}) was set equal to the measured value (1.1 dS m^{-1}). At the end of the simulation, Eq. (9) was used to convert the simulated EC_{sw} values to EC_e, which allowed for comparison with measured values.

Solute entering the soil system was described using a third-type (or flux type) boundary condition at the porous clay pipe wall. No solute was assumed to be taken up by the plants. A Neumann boundary condition for solute transport was used at the bottom of the soil profile. For the simulations we used a longitudinal dispersivity equal to one-tenth of the depth of the flow domain (i.e. $\varepsilon_L = 10$ cm), which is consistent with various studies indicating that ε_L is about one-tenth the scale of a transport experiment (Beven et al., 1993; Cote et al., 2003; Phogat et al., 2011). The transversal dispersivity (ε_T) was assumed to be one-tenth of the longitudinal dispersivity (e.g., Hanson et al., 2006).

The model of Feddes et al. (1978) modifies root water uptake depending on the water status of the soil and is parameterized in terms of four pressure head values, $h_1 > h_2 > h_3 > h_4$. The parameterization is such that uptake occurs at the potential rate when the pressure head is in the optimal range $h_3 \le h \le h_2$, drops off linearly when $h > h_2$ or $h < h_3$, and becomes zero when $h \le h_4$ or $h \ge h_1$. The parameter h_3 is expected to be a function of the

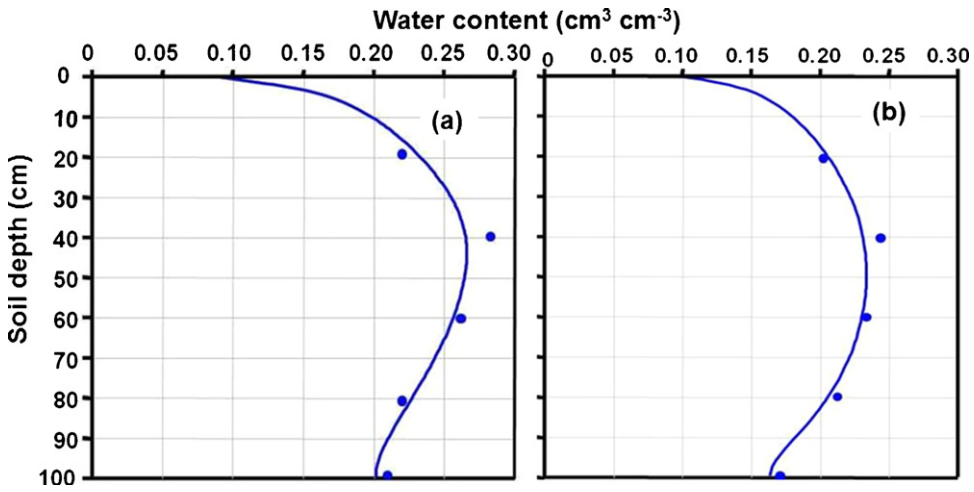

Fig. 5. Water content in the soil profile at the end of the 60 days crop season. (a) 20 cm from the centre of the pipe and (b) 60 cm from the centre of the pipe.

evaporative demand. HYDRUS permits the specification of high (h_{3high}) and low (h_{3low}) values of this parameter for high (rH) and low (rL) potential transpiration rates, respectively. An interpolation scheme is further used to determine h_3 for intermediate conditions (Šimůnek et al., 1999). For our simulations, we used literature values for beans (which are similar to okra): $h_1 = -10$ cm, $h_2 = -25$ cm, h_{3high}, $= -750$ cm, $h_{3low} = -2000$ cm, $h_4 = -8000$ cm, $rH = 0.5$ cm d^{-1}, and $rL = 0.1$ cm d^{-1}. The okra root distribution in the soil profile was described using the model of Vrugt et al. (2001) with roots extending 20 cm laterally and 60 cm vertically.

2.3. Evaluation of model predictions

The agreement of HYDRUS-2D model predictions with the measured data was quantified in terms of three statistical measures: the mean bias error (*MBE*), the root mean square error (*RMSE*), and the coefficient of determination (R^2). These parameters are defined as (Willmott, 1982):

$$MBE = \frac{\sum_{i=1}^{n}(P_i - O_i)}{n} \quad (10)$$

$$RMSE = \sqrt{\frac{\sum_{i=1}^{n}(P_i - O_i)^2}{n}} \quad (11)$$

$$R^2 = 1 - \frac{\sum_{i=1}^{n}(P_i - O_i)^2}{\sum_{i=1}^{n}(O_i - \bar{O})^2} \quad (12)$$

where n is the number of data points; P_i is the ith predicted data point; O_i is the ith observed data; and $\bar{O}$ is the mean of observed data. *MBE* can identify potential bias (i.e., underestimation and overestimation) in the predicted values, whereas *RMSE* and R^2 give overall measures of the goodness-of-fit.

3. Results and discussion

Fig. 4 shows water particle trajectories originating from the pipe wall after 3 days of irrigation. The trajectories provide a clear illustration of the direction of water movement from the clay pipe into the medium-textured soil. Again, in this system, water moves not only downward due to gravity but also upward as a result of capillarity, surface evaporation, and, to a lesser extent, the applied pressure head. Water moving upward is either used by plants to meet transpiration, or lost to the atmosphere while leaving the salts

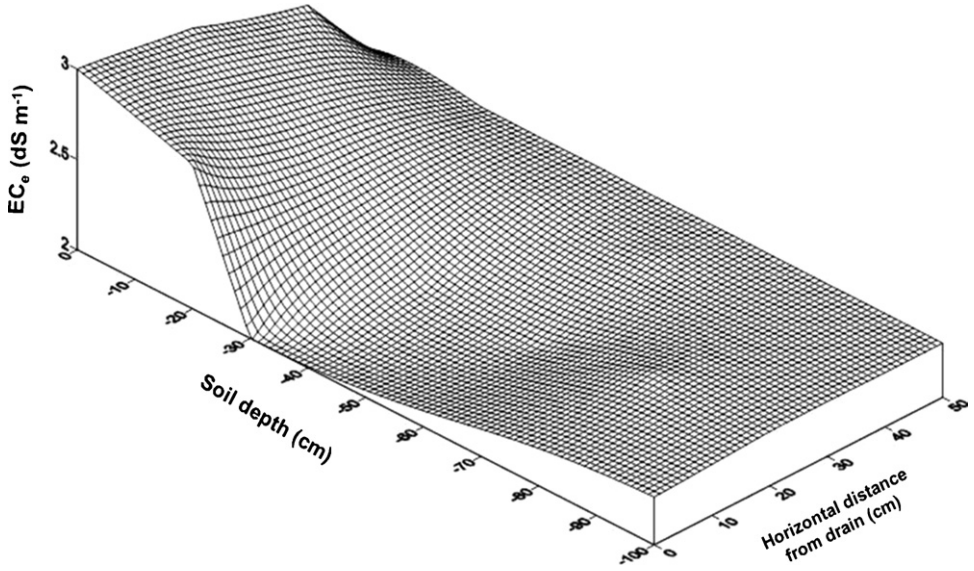

Fig. 6. Simulated distribution of salt (EC_e) in loamy soil after 60 days crop season.

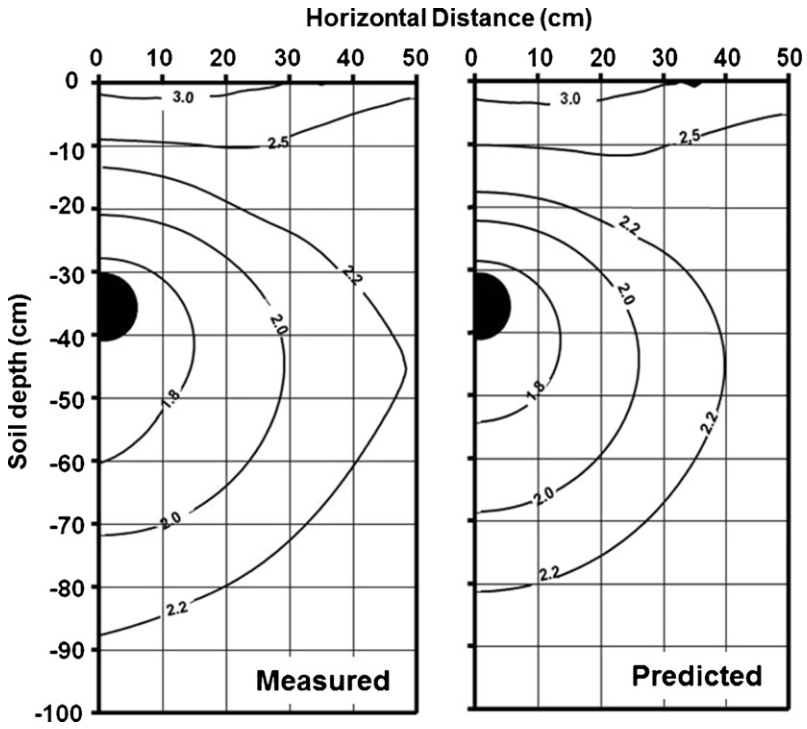

Fig. 7. Measured and predicted electrical conductivity of soil saturated extract (EC_e) after 60 days of irrigation.

in the soil. Because of evaporation, the soil water content decreases significantly near the soil surface, as shown in Fig. 5.

Fig. 6 shows the computed distribution of salt (EC_e) within the root zone after the 60 days okra growing season. Results show relatively high salt concentrations above the clay pipe near the soil surface and within the root zone, but lower concentrations near the clay pipe at 30 cm depth. Fig. 7 compares predicted and measured EC_e values at the end of the growing season. Results clearly indicate salt accumulation near the wetting front laterally, as well as accumulation of salt at or near the soil surface. Measured and simulated salinity patterns are nearly identical, with salinity increasing with distance from the pipe, and being highest at the soil surface. Similar salinization patterns were also reported by Morvant et al. (1997), Cox (2001), Badr and Taalab (2007), Lamm et al. (2007) and Trenton et al. (2008) for subsurface drip irrigation.

Fig. 8 shows computed soil water contents and EC_e values versus time at different soil depths 20 cm laterally away from the centre of the clay pipe. The plots show that the soil water content at a depth of 5 cm initially decreases to about 0.09 $cm^3 cm^{-3}$ because of surface evaporation, but then the wetting front arrives and the water content increases to approximately 0.15 and 0.17 $cm^3 cm^{-3}$ after 30 and 60 days, respectively. At the same 5 cm depth, EC_e initially increases from 2.3 to 2.6 dS m^{-1} after 9 days of irrigation, but then gradually decreases to 2.4 dS m^{-1}, before again increasing to 2.9 dS m^{-1}. In contrast, the soil water content at the 35 cm soil depth rapidly increases to 0.23 $cm^3 cm^{-3}$ after 2 days of irrigation and thereafter slowly climbs to around 0.29 $cm^3 cm^{-3}$, while the corresponding EC_e gradually decreases to 1.8 dS m^{-1} after 60 days of irrigation. At 90 cm, the soil water content remains unchanged until the arrival of the wetting front after about 30 days, and then gradually increases to 0.27 $cm^3 cm^{-3}$ after 60 days. Similarly, EC_e remains unchanged for 30 days and then gradually decreases to a little less than 2.0 dS m^{-1} after 60 days.

In all, the results in Figs. 7 and 8 indicate that salts accumulate predominantly near the soil surface. This accumulation of salt near the soil surface after one growing season can adversely affect the germination and emergence of a new crop. Knowledge of salt

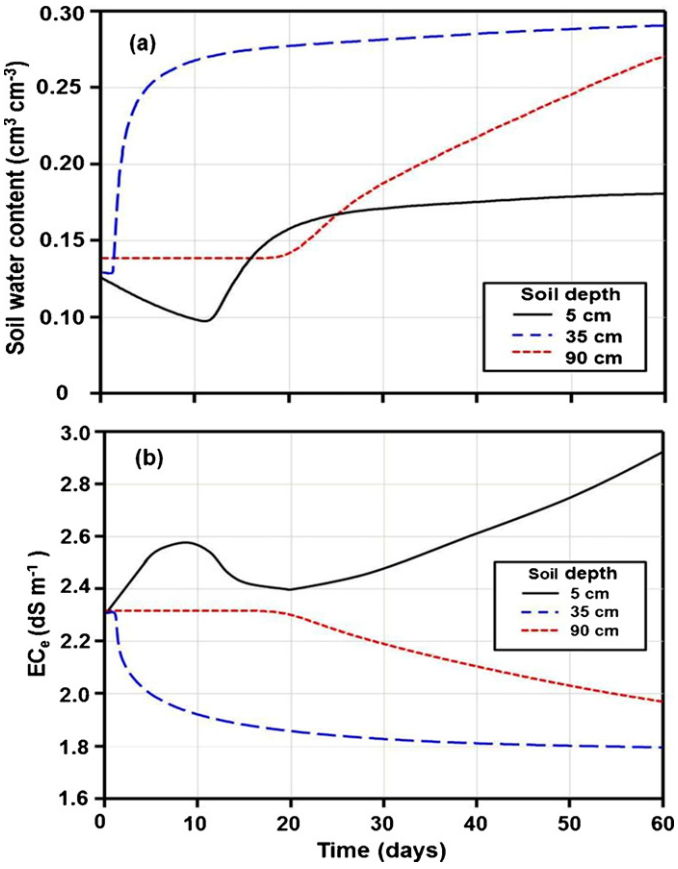

Fig. 8. Computed change in (a) soil water content ($cm^3 cm^{-3}$) and (b) electrical conductivity of soil saturated extract (EC_e) against time at different soil depths in a profile located at 20 cm from the centre of the pipe.

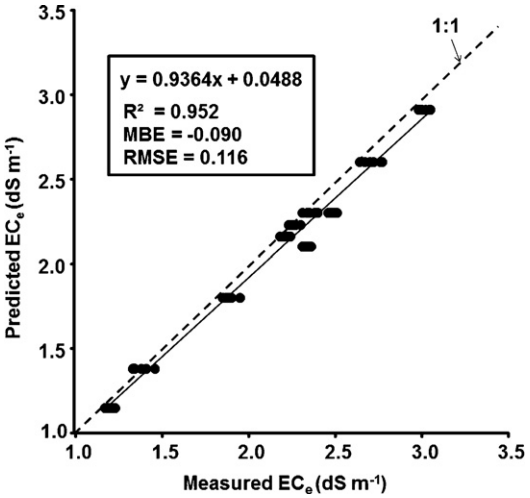

Fig. 9. Correlation of measured and predicted end-of-season saturation paste electrical conductivity (EC_e) at different depths in the soil profile at lateral distances of 20 and 40 cm from the centre of the pipe.

distributions at the end of a growing season would allow producers more flexibility in managing salt accumulation, and could eliminate operating cost associated with unnecessary soil leaching.

Fig. 9 shows a comparison of predicted end-of-season EC_e values with values measured for different soil depths (0–20, 20–40, 40–60, 60–80 and 80–100 cm) at lateral distances of 20 cm and 40 cm from the centre of pipe, at 3 locations along the pipe. The results show a strong relationship between observed and simulated values ($R^2 = 0.952$, a slope close to one, and an intercept near zero). Based on the goodness-of-fit parameters (*MBE*, *RMSE*, R^2) in Fig. 9 and a visual inspection of the agreement between the simulated and measured values, we conclude that the salt distribution in the soil profile following subsurface porous clay pipe irrigation could be predicted well using HYDRUS-2D. The results provide support for using HYDRUS-2D as a useful tool for investigating, designing and managing subsurface clay pipe irrigation systems.

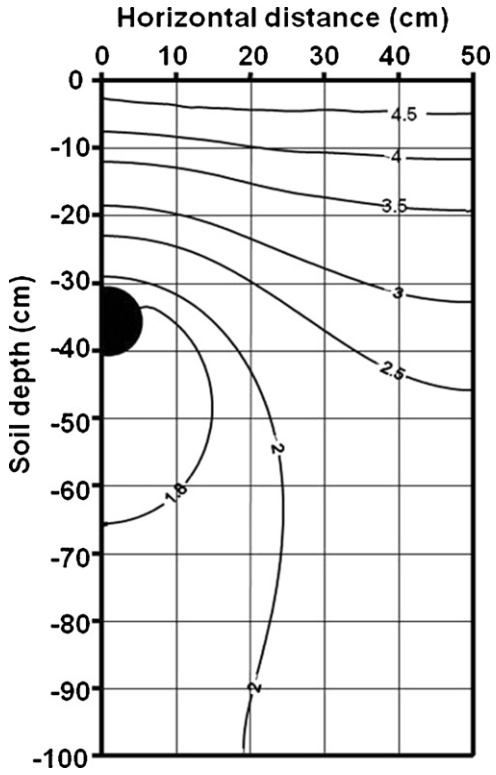

Fig. 10. Predicted electrical conductivity (EC_e) of soil saturated extract of the soil profile after 2 years of irrigation.

In order to determine the long term effect of subsurface clay pipe irrigation on salt distributions, HYDRUS-2D was used to simulate salt distributions assuming beans were grown on the same soil for two years. Simulation results (Fig. 10) show that two years of continuous irrigation with the subsurface clay pipe system leads to further salinization of soil profile above the clay pipe: the EC_e increased to approximately 5 dS m^{-1} near the soil surface. However, the salt concentration below the pipe decreased to 1.8 dS m^{-1}. The relatively high near-surface-salinity predicted after two years indicates a need for leaching salts from the soil profile before establishing a new crop. This then requires surface water applications unless occasional rain alleviates the salt accumulation problem.

4. Conclusion

Salt accumulation in soil due to subsurface porous clay pipe irrigation was studied experimentally and by means of HYDRUS-2D numerical simulations. An okra crop was grown on a loam soil with an initial soil salinity of $EC_e = 2.3$ dS m^{-1}. The subsurface clay pipe irrigation system was installed at 30 cm depth and the irrigation water had a salinity of $EC_{iw} = 1.1$ dS m^{-1}. Both measured and predicted soil salinity patterns showed higher soil salinity in the soil profile above the clay pipe, and lower salinity around the clay pipe lateral. A strong relationship existed between observed and simulated salinity values ($R^2 = 0.952$, slope close to one, intercept near zero), although overall the model tended to somewhat underestimate the measured values. In arid regions it may be necessary to use occasional surface water application to leach salts from the surface soil, especially during the initial stages of the growing season when crops are typically most sensitive to salinity. The results suggest that HYDRUS-2D can be used as a useful tool for investigating, designing and management of subsurface clay pipe irrigation systems.

Acknowledgment

The Higher Education Commission (HEC) of Pakistan is gratefully acknowledged for funding the project “Use of subsurface irrigation system to meet the water crisis in the country” under the National Research Program for Universities (NRPU).

References

Abu-Zreig, M., Atoum, F.M., 2004. Hydraulic characteristics of clay pitchers produced in Jordan. Can. Biosyst. Eng. 46 (1), 15–20.
Allen, R.G., Pereira, L.S., Raes, D., Smith, M., 1998. Crop evapotranspiration. Guidelines for computing crop water requirements. Irrigation and Drainage. Paper No. 56. FAO, Rome, Italy.
Ashrafi, S., Gupta, A., Singh, M.B., Izumi, N., Loof, R., 2002. Simulation of infiltration from porous clay pipe in subsurface irrigation. Hydrological Sciences Journal 47 (2), 253–268.
Badr, M.A., Taalab, A.S., 2007. Effect of drip irrigation and discharge rate on water and solute dynamics in sandy soil and tomato yield. Australian Journal of Basic and Applied Science 1 (4), 545–552.
Bear, J., 1972. Dynamics of fluids in porous media. Elsevier, New York.
Beven, K.J., Henderson, D.E., Reeves, A.D., 1993. Dispersion parameters for undisturbed partially saturated soil. Journal of Hydrology 143, 19–43.
Cote, C.M., Bristow, K.L., Charlesworth, P.B., Cook, F.J., Thorburn, P.J., 2003. Analysis of soil wetting and solute transport in subsurface trickle irrigation. Irrigation Science 22, 143–156.
Cox, D.A., 2001. Growth, nutrient content and growth medium electrical conductivity of poinsettia irrigated by sub irrigation or from overhead. Journal Plant Nutrition 24, 523–533.

Craze, B., Holman, G., Chapman, G.A., Stone, M.J., 2003. Soil survey standard test methods. Dep. of Land and Water Conservation, Sydney, NSW, Australia.
Feddes, R.A., Kowalik, P.J., Zaradny, H., 1978. Simulation of field water use and crop yield. In: Simulation Monographs. Pudoc, Wageningen, The Netherlands.
Hanson, B.R., Simunek, J., Hopmans, J.W., 2006. Evaluation of urea-ammonium-nitrate fertigation with drip irrigation using numerical modeling. Agricultural Water Management 86, 102–113.
Hanson, B.R., Bendixen, W.E., 1995. Drip irrigation controls soil salinity under row crops. California Agriculture 49 (4), 19–23.
Hanson, B.R., 2003. Drip irrigation increases tomato yields in salt-affected soil of San Joaquin Valley. California Agriculture 57, 132–137.
Hussain, G., Al-Jaloud, A.A., Al-Shammary, S.A., Karimulla, S., Al-Aswad, S.O., 1997. Effect of saline irrigation on germination and growth parameters of barley (*Hordeum vulgare* L.) in a pot experiment. Agricultural Water Management 34, 125–135.
Jiménez-Martinez, J., Skaggs, T.H., van Genuchten M.Th. Candela, L., 2009. A root zone modelling approach to estimating groundwater recharge from irrigated areas. Journal of Hydrology 367, 138–149.
Lamm, F.R., Ayars, J.E., Nakayama, F.S., 2007. Micro-irrigation for crop production: design, operation, and management. Development in Agricultural Enginerring, vol. 13. Elsevier, UK, p. 147.
Mer, R.K., Prajith, P.K., Pandya, D.H., Pandey, A.N., 2000. Effect of salts on germination of seeds and growth of young plants of *Hordeum vulgare*, *Triticum aestivum*, *Cicer arietinum* and *Brassica juncea*. Journal of Agronomy and Crop Science 185, 209–217.
Morvant, J.K., Dole, J.M., Allen, E., 1997. Irrigation systems alter distribution of roots, soluble salts, nitrogen and pH in the root medium. Horticulture Technology 7, 156–160.
Pachepsky, Y.A., Smettem, K.R.J., Vanderborght, J., Herbst, M., Vereecken, H., Wosten, J.H.M., 2004. Reality and fiction of models and data in soil hydrology. In: Feddes, R.A., et al. (Eds.), Unsaturated-Zone Modeling. Kluwer Academic Publishers, Dordrecht, the Netherlands.
Phogat, V., Mahadevan, M., Skewes, M., Cox, J.W., 2011. Modelling soil water and salt dynamics under pulsed and continuous surface drip irrigation of almond and implications of system design. Irrigation Science 30 (4), 315–333.
Qiaosheng, S., Zuoxin, L., Zhenying, W., Haijun, L., 2007. Simulation of the soil wetting shape under porous pipe sub-irrigation using dimensional analysis. Irrigation and Drainage 56, 389–398.
Roberts, T.L., Lazarovitch, N., Warrick, A.W., Thompson, T.L., 2009. Modeling salt accumulation with subsurface drip irrigation using HYDRUS-2D. Soil Science Society of America Journal 73, 233–240.
Schaap, M.G., Leij, F.J., van Genuchten, M.Th., 2001. ROSETTA: a computer program for estimating soil hydraulic properties with hierarchical pedotransfer functions. J. Hydrol. 251, 163–176.
Šimůnek, J., Sejna, M., van Genuchten, M.Th., 1999. The HYDRUS-2D Software Package for Simulating The Two-Dimensional Movement of Water, Heat, and Multiple Solutes in Variably-Saturated Media. IGWMC-TPS 53, Version 2.0, International Ground Water Modeling Centre. Colorado School of Mines, Golden, CO.
Šimůnek, J., van Genuchten, M.Th., 2008. Modeling non equilibrium flow and transport with HYDRUS. Vadose Zone Journal 7 (2), 782–797.
Šimůnek, J., Bradford, S.A., 2008. Vadose Zone Modeling: Introduction and importance. Vadose Zone Journal 7 (2), 581–586.
Siyal, A.A., van Genuchten, M.Th, Skaggs, T.H., 2009. Performance of pitcher irrigation systems. Soil Science 174 (6), 312–320.
Siyal, A.A., Skaggs, T.H., 2009. Measured and simulated wetting patterns under porous clay pipe subsurface irrigation. Agricultural Water Management 96 (6), 893–904.
Trenton, L.R., Scott, A.W., Arthur, W.W., Thomas, L.T., 2008. Tape depth and germination method influence patterns of salt accumulation with subsurface drip irrigation. Agricultural Water Management 95 (6), 669–677.
U.S. Salinity Laboratory Staff, 1954. Diagnosis and improvement of saline and alkali soils. Handbook, vol.60. U.S. Dept. Agriculture, U.S. Government Printing Office, Washington, DC, p. 160.
van Genuchten, M.Th., 1980. A closed-form equation for predicting the hydraulic conductivity of unsaturated soils. Soil Science Society of America Journal 44, 892–898.
Vrugt, J.A., Hopmans, J.W., Simunek, J., 2001. Calibration of a two-dimensional root water uptake. Soil Science Society of America Journal 65, 1027–1037.
Willmott, C.J., 1982. Some comments on the evaluation of model performance. Bulletin of the American Meteorological Society. 63 (11), 1309–1313.